Proceedings of ASME Turbo Expo 2011
GT2011
June 6-10, 2011, Vancouver, British Columbia, Canada

GT2011-46841

Optimization of Power Train Involving Gas Turbine Driven Compressors and Aerial Coolers

K.K. Botros*
NOVA Research & Technology Center
2928 – 16 Street NE
Calgary, Alberta, Canada
Email: botrosk@novachem.com
* Corresponding Author

H. Golshan
TransCanada PipeLines Limited
111 - 5 Avenue SW
Calgary, Alberta, Canada
Email: hossein_golshan@transcanada.com

A. Hawryluk
NOVA Research & Technology Center
2928 – 16 Street NE
Calgary, Alberta, Canada
Email: hawryla@novachem.com

B. Sloof
Calgary, Alberta, Canada
TransCanada PipeLines Limited
111 - 5 Avenue SW
Calgary, Alberta, Canada
Email: brian_sloof@transcanada.com

ABSTRACT

Multi-objective optimizations were conducted for a compressor station comprising two dissimilar compressor units driven by two dissimilar gas turbines, two coolers of different size, and two parallel pipeline sections to the next station. Genetic algorithms were used in this optimization along with models describing the performance characteristics of gas turbines, compressors, aerial coolers, and downstream pipeline section. Essential in these models is the heat transfer between the gas and soil as it affects the pressure drop along the pipeline, and hence relates back to the coolers and compressor flow/pressure settings. Further investigative techniques were developed to also minimize NOx and CO2e emissions along with total energy consumption, i.e. fuel (used in the driver gas turbines) and electrical energy (used in the electrical fans of the aerial coolers).

Two optimization scenarios were conducted: 1) Two-objective optimization of total energy consumption and NOx emission, and 2) Two-objective optimization of total energy consumption and CO2e emission. The results showed that savings in the energy consumption in the order of 5–6% is achievable with slight adjustment to unit load sharing and coolers by-pass/fan speed selections. It appears that most of the savings (around 70–75%) are derived from optimizing the load sharing between the two parallel compressors, while the balance of the savings is realized from optimizing the aerial coolers settings. In order to optimize operation for minimum NOx emission as well, a shift towards employing more of the aerial coolers is required. Preliminary cost analysis was conducted for valuation of balancing between energy consumption vs. emission loading in terms of both NOx and CO2e.

NOMENCLATURE

C_P	= *specific heat capacity at constant pressure*
D	= *pipe diameter*
e	= *total energy consumption*
f	= *friction factor*
H	= *adiabatic head across a compressor unit*
$\dot{m}$	= *mass flow rate*
N	= *compressor speed*
P	= *pressure*
Q	= *actual inlet flow rate to a compressor unit*
T	= *temperature*
U	= *overall heat transfer coefficient*
W	= *compressor power*

Greek Letters:

α = *constant*
η_{is} = *compressor isentropic efficiency*
η_m = *compressor shaft mechanical efficiency*
η_{th} = *turbine thermal efficiency (inverse of heat rate)*
φ = *pipeline hydraulic function*
ρ = *fluid density*

Subscripts:

1-4 = *locations in the system (see Fig. 1)*
amb,∞ = *ambient condition*
i = *inside of pipe*
j,k = *compressor or cooler identifier*
min = *minimum*
max = *maximum*
o = *outside of pipe*
soil = *soil condition*

INTRODUCTION

The TransCanada system may be described as a collection of measurement, pipeline, compressor station, and valve facilities of every size, type, vintage, design, and configuration imaginable. This is not much different than many large pipeline systems worldwide which are always faced with the significant challenge associated with optimization. However, the Alberta system is somewhat unique in terms of throughput (285–343 10^6 m^3/day) and linepack (370–430 10^6 m^3), which cannot be influenced by TransCanada, but rather by the extreme climatic conditions (-40 to 40°C), soil conditions (some frozen areas) and a diversity of maximum allowable operating pressure (MAOP) that varies between 2750 to 9930 kPa-g.

In previous work by TransCanada, Genetic Algorithm (GA)-based optimization methodology was used to perform automated optimizations specifically to its Alberta System. The outcome of this effort was successfully implemented and was reported in the open literature [1-5].

In the aforementioned development, high level performance characteristics were used to model the major components in the compressor stations, namely the compressor units, drivers and aerial coolers. These models employed 'unit-operation' type models without accounting for details of load sharing, variation in the turbine heat rates with loads, aerial cooler by-pass and fan speed control, etc. This was found to be not only appropriate but proved to be sufficient when a system network comprising 22 compressor stations and 54 decision variables, hence an optimization space of 1.85×10^{78} cases was analyzed [1].

Since this work, an opportunity was recognized for further optimization to achieve more savings in energy consumption. In multi-unit compressor stations comprising dissimilar compressor units, dissimilar gas turbine drivers, multi-coolers with possibility of controlled cooler by-pass and fan speed setting, it is realized that optimization of this station configuration could trigger more saving in energy use. The system to be optimized in this case would start from the gas turbine drivers, booster compressors, coolers, and downstream pipeline section to the next compressor station. Such a system would be considered a subsystem of a larger network which was analyzed in the previous work [1-4]. Once this subsystem is optimized, it can be used as sub-module in a larger optimization of a multi-station network. We called the optimization of such a sub-system: "*optimization of power train*", comprising all of the elements listed above.

This paper presents the methodology adopted for such optimization which is still based on GA with the familiar constraints of booster compressor operating boundaries, gas turbine performance limits, and climatic conditions. An example of two dissimilar units from a compressor station on the TransCanada system driven by dissimilar gas turbines (LM1600 and LM 2500) as well as two different size coolers was considered to demonstrate the optimization approach. Results include two-objective optimization to minimize energy consumption (or cost) and NOx emission for a given throughput. Alternate two-objective optimization involves minimization of carbon dioxide equivalent (CO2e) and NOx emission, also for a given throughput. Preliminary cost analysis was conducted for valuation of balancing between energy consumption vs. emission loading in terms of both NOx and CO2e.

OPTIMIZATION METHODOLOGY

Typically, there are three fundamental objective functions pertaining to a gas pipeline network operation. These are total energy consumption (or cost), throughput and linepack. The present paper deals with all three objectives in addition to optimization of single- vs. multi-compressor unit operations. For example, optimization of the energy consumption can be formulated as follows:

$$\min\left\{\sum_{r\in R} e\left(\dot{m}, P_s, P_d\right)_r + \sum e(fans)\right\} \tag{1}$$

subject to the following constraints:

$$\left.\begin{array}{r} W_{r,\min} < W < W_{r,\max} \\ N_{r,\min} < N_r < N_{r,\max} \\ Surge < \left(\dfrac{Q}{N}\right)_r < Stonewall \end{array}\right\} r \in R \tag{2}$$

and other linear and non-linear constraints, where:

$$e(\dot{m}, P_s, P_d)_r = \alpha \frac{\dot{m}H}{\eta_{is}\eta_m\eta_{th}}, \forall(\dot{m}, P_s, P_d) \in D \tag{3}$$

Maximum throughput (delivery or receipt), can be represented by:

$$\max\left\{\sum_{k=1}^{N_D} Q_k\right\} \quad ; \quad \max\left\{\sum_{k=1}^{N_R} Q_k\right\} \tag{4}$$

In the case of minimizing energy consumption for gas pipeline systems, often multiple unit compressor stations present significant challenges to the optimization tool. This is because several feasible solutions might exist which satisfy both the minimum objective function and associated constraints. Local minima might occur leading to a non-convexity optimization problem [6,7]. Therefore, a detailed station optimization tool (like the one used in the present work) should be incorporated in the overall system optimization to arrive at the optimum solution of station operation for a given set of control parameters.

Gradient-based optimization methods have been used to analyze gas pipeline networks in the past [8-14]. Like the name implies, they rely on the derivative of the function being optimized with respect to all control variables that define the system. The derivative, or slope, of the function at a sampled point determines the direction in which the algorithm will progress in the operating space. There are several gradient-based optimization methods depending on the nature of the objective function and associated constraints, i.e. constrained and unconstrained linear, quadratic and non-linear programming. An extensive review of these methods and available software tools can be found in [15]. Applications of these methods to steady-state pipeline optimization were found to be unstable [8], particularly close to the operation boundaries, often trapped in local minimum and very dependent on the initial (starting) point. These methods have also been extended to transient pipeline optimization [16-18], however only on relatively smaller systems. Optimizations based on dynamic programming have been attempted, e.g. those based on Bellman's Optimality Principle [19-21], again limited only to pipelines with series stations.

The other category of optimization methods is based on stochastic methods such as Recourse Methods, Simulated Annealing and Genetic Algorithm (GA). However, GA has great advantages for large systems with many interlinked control variables and a large number of possible cases (hence large search space). As the algorithm evolves through generations (similar to iterations in a typical algorithm), the objective function trends towards an optimum value. Due to the pseudo-random nature of the algorithm and its independence from objective function gradients, it does not become fixed in a local optimum point.

The first application of GA to pipeline optimization was introduced by Goldberg and Kuo [22,23] where they demonstrated its application on a liquid pipeline system. They demonstrated that GA's are computationally more demanding than conventional optimization algorithms, but offer many advantages over conventional methods. Current development involves hybrid optimizations, which combines the advantages of both categories of optimization methods [24].

As mentioned earlier, multiple unit compressor stations could produce many local minima, but there is a fundamental requirement to find the global minimum regardless of the initial starting point. Secondly, multi-objective requirements, robustness and stability of the optimization procedure while managing the computational times, suggested that GA would best suit optimization of the power train system under consideration in the present work.

COMPRESSION POWER TRAIN SYSTEM

A two-unit compressor station on the TransCanada System is considered as an example of a complex power train system. It comprises two dissimilar compressor units driven by two dissimilar gas turbines as shown in Table 1. The station includes two aerial coolers of different sizes (termed J and K), which are connected in parallel to both of the compressor units. The downstream section of the pipeline to the next station (69.5 km downstream) is composed of two parallel lines of different sizes, one of which is looped. Figure 1 shows a schematic of the station and the downstream pipeline section which comprises the power train system considered as an example for the present optimization exercise.

TABLE 1: TWO DISSIMILAR COMPRESSOR AND GAS TURBINE DRIVERS.

Unit	Compressor Unit	Driver
J	DeLaval B30/30	LM 1600
K	PGT PCL-802/N	LM2500

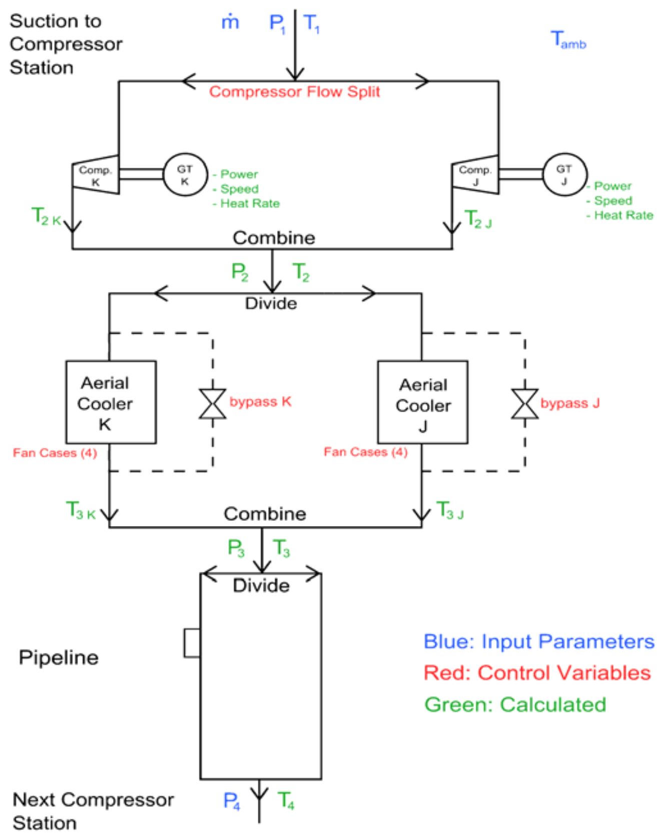

FIGURE 1: SCHEMATIC OF THE TWO-UNIT COMPRESSOR STATION AND DOWNSTREAM PIPELINE SECTION UNDER STUDY.

Table 2 gives salient specifications of these aerial coolers, and their dimensionless performance characteristics in terms of pressure drop and degree of cooling are given in Figures 2 through 6. The pressure drop is normalized to the density of the fluid and fitted to a polynomial function, while the degree of cooling is normalized with respect to the fluid temperatures depicted in Figure 2, and fitted to the following function:

$$\frac{T_{in} - T_{out}}{T_{in} - T_{\infty}} = f(\dot{m}) = \frac{1 + a\dot{m}}{1 + b\dot{m} + c\dot{m}^2} \quad (5)$$

TABLE 2: SPECIFICATIONS OF THE TWO AERIAL COOLERS.

Aerial Cooler	J	K
NO. OF PASSES	1	1
NO. OF BAYS	6	6
BARE SURFACE AREA/BAY (m2)	427.68	408.6
NO. OF FANS PER BAY	2	2
FAN DRIVE TYPE	Two Speeds	Two Speeds
MAX FAN SPEED (RPM)	201	245
MIN FAN FRACTION (RPM)	50% of max	50% of max
AIR FLOW/FAN at 100% speed (kg/s)	69	115.9
Tube Materials	SA-334-6	SA-334-7
Fin Materials	Aluminum	Aluminum
Tube Length (m)	14.63	12.19
Fan Power (DESIGN) (kW) - for one fan	8.5	20.1
Fan Power (MOTOR) (kW) - for one fan	14.9	29.8
NO. OF BUNDLES OF TUBES PER BAY	1	2
NO. OF TUBES PER BAY	293	420
TUBE O.D (mm)	31.75	25.4
TUBE WALL THICKNESS (mm)	1.65	1.65
TUBE I.D (mm)	28.45	22.1

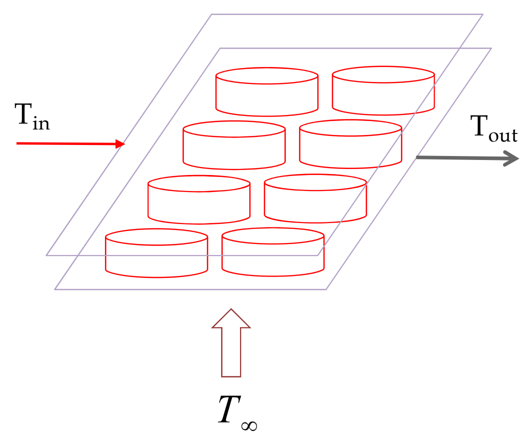

FIGURE 2: AERIAL COOLER TEMPERATURE NOMENCLATURE.

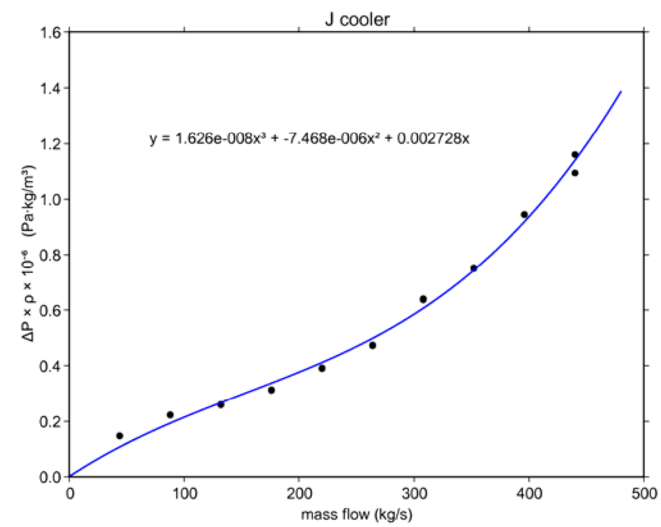

FIGURE 3: NORMALIZED PRESSURE DROP THROUGH COOLER J

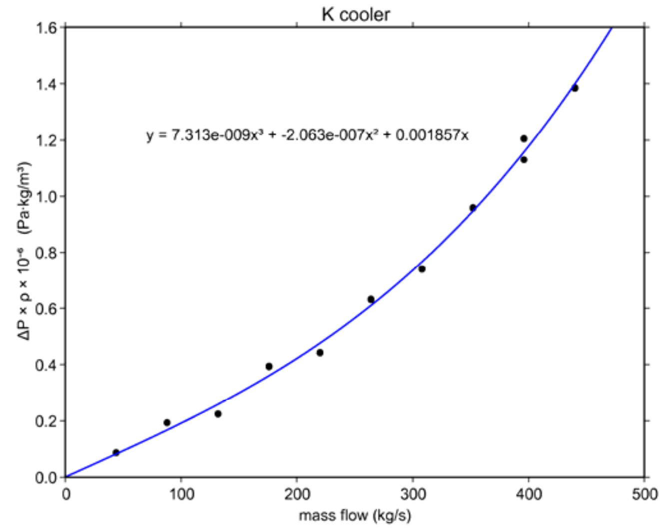

FIGURE 5: NORMALIZED PRESSURE DROP THROUGH COOLER K.

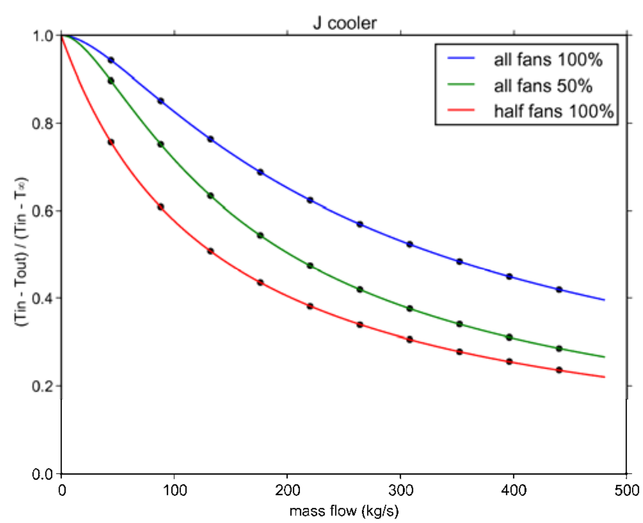

FIGURE 4: DIMENSIONLESS PERFORMANCE CHARACTERISTICS OF COOLER J.

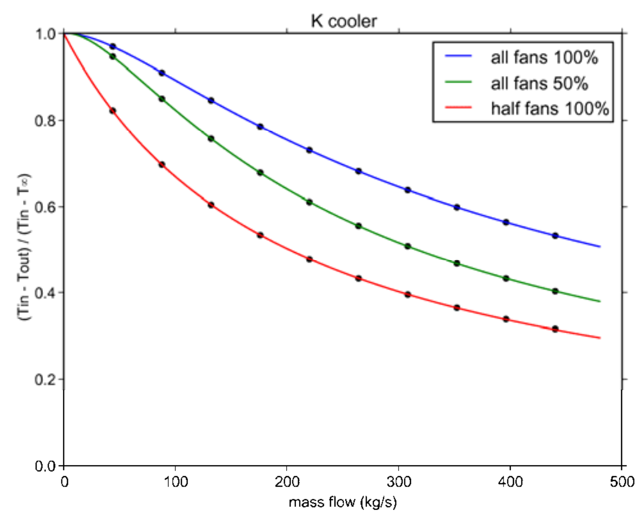

FIGURE 6: DIMENSIONLESS PERFORMANCE CHARACTERISTICS OF COOLER K.

The downstream section of the pipeline to the next station (69.5 km downstream) is composed of two parallel lines of different sizes, one of which is looped as shown in Fig. 7. The compressor performance characteristics and associated driver's heat rate map at ambient temperature = 10°C are shown in Figs. 8 and 9, respectively. Notice that the range of the flow capacity of unit K is approximately twice that of unit J.

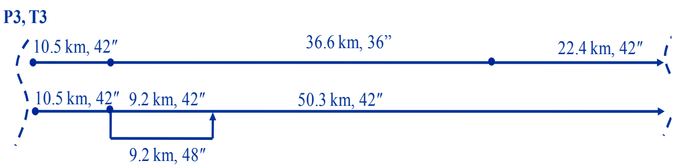

Pipe	36″	42″	48″
Heat transfer coefficient (W/m².C)	4.42	4.04	3.6
ID (mm)	891.8	1046	1195
Internal Surface Roughness (μm)	5.08	5.08	6.35

FIGURE 7: SCHEMATIC AND DIMENSIONS OF THE TWO PARALLEL PIPELINE SECTIONS DOWNSTREAM OF THE COMPRESSOR STATION.

A custom-built computer program (Simulator) was used for hydraulic modeling of the power train and downstream pipeline section described above. The model simulates the steady-state gas flow from the suction to the J and K compressors to the downstream end of the pipeline section (i.e. to the next compressor station). The model is non-isothermal; it calculates the gas temperature variations across the aerial coolers and along the pipeline section and account for the heat exchange between the pipe and the ground. The pressure drop and temperature profile along the various pipeline sections are obtained from solving:

$$\frac{dP}{dx} = -\frac{16 f \, \dot{m}^2}{\pi^2 \rho D_i^5} \tag{6}$$

and

$$\frac{dT}{dx} = -\frac{U \pi D_o}{\dot{m} C_p}(T - T_{soil}) \tag{7}$$

The temperature increase in a compressor is modeled as an irreversible adiabatic process. Upon mixing of streams of different temperatures at the discharge from both compressor units, downstream of the coolers and cooler by-passes, the mixed temperature is calculated using conservation of enthalpy. The American Gas Association Report No. 8 (AGA-8) equation of state [25] is used in determining the various physical and thermodynamic properties at each condition of the gas, given the prevailing gas mixture composition shown in Table 3.

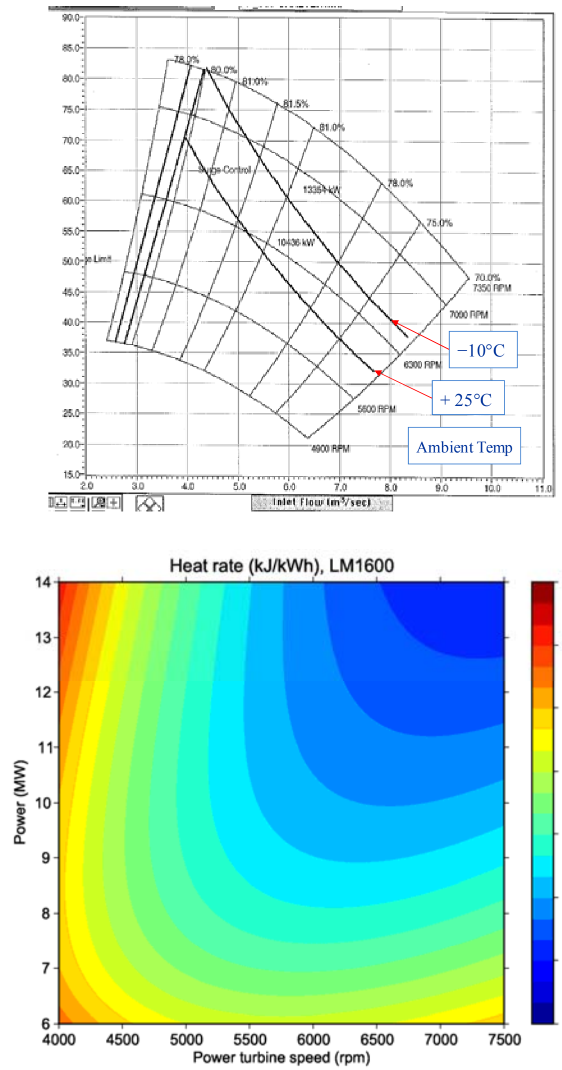

FIGURE 8: PERFORMANCE CHARACTERISTICS OF THE J COMPRESSOR AND ITS GAS TURBINE DRIVER AT 10°C AMBIENT TEMPERATURE.

In a single-objective optimization for a given throughput, case-specific input parameters are (see Fig. 1 for notation):

P_1, P_4, T_1, T_{soil}, T_{amb}, total gas flow

The values for these parameters are given in Table 4.

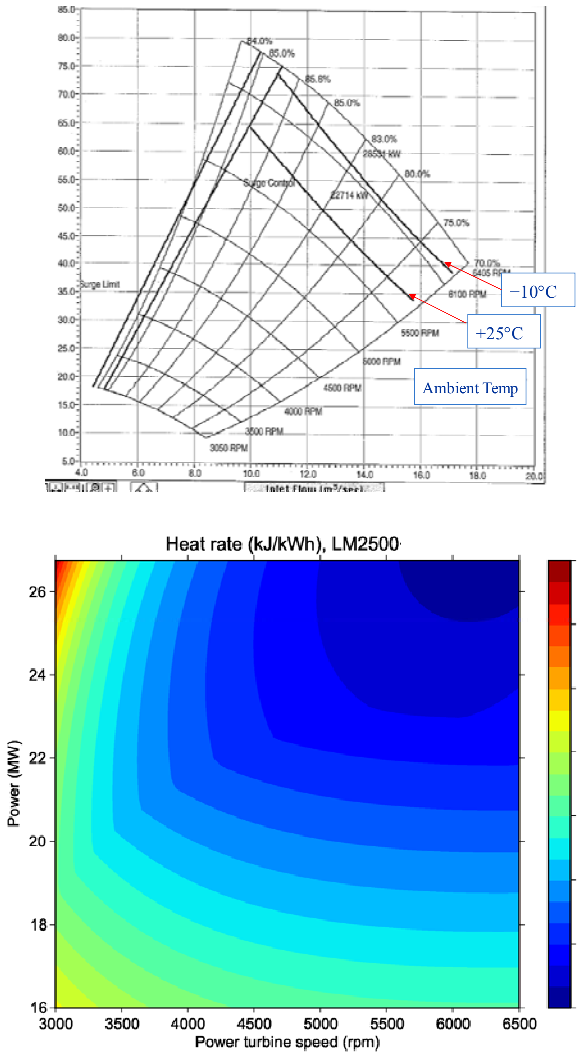

FIGURE 9: PERFORMANCE CHARACTERISTICS OF THE K COMPRESSOR AND ITS GAS TURBINE DRIVER AT 10°C AMBIENT TEMPERATURE

TABLE 3: GAS MIXTURE COMPOSITION.

	Mole %
C1	95.68766
C2	2.645223
C3	0.164775
i-C4	0.010543
n-C4	0.011128
i-C5	0.003811
n-C5	0.002448
C6	0.003521
C7	0.000498
C8+	0.000124
N2	0.945524
CO2	0.496869
HE	0.027879
	100.000

TABLE 4: INPUT PARAMETERS FOR THE POWER TRAIN SYSTEM OF FIG. 1.

Input Parameters		
Suction Pressure (P_1)	4250	kPa-a
Suction Pressure at Next Ststion (P_4)	4250–5000	kPa-a
Suction Temperature (T_1)	10	°C
Soil Temeprature	10	°C
Ambient Temeprature	10	°C
Gas Flow	400–650	kg/s

The control variables are:

- Compressor load sharing in terms of the mass flow split to each compressor unit.
- Four possible aerial cooler fan speed settings for each of the J and K coolers, namely i) all fans are running at 100%, ii) all fans are running at 50% speed, iii) half the number of fans are running at 100% speed, and iv) all fans are turned off.
- Aerial cooler fraction of the gas bypassing the respective cooler.

Table 5 gives the selected resolution for each of the above control variables, the range, and the corresponding required number of GA strings. It is shown that for the two-objective exercise, the total number of GA strings is 39 and the resulting search space is 5.5 x 10^{11}. This large search space makes any unorganized search of all configurations for the best case impossible.

TABLE 5: CONTROL VARIABLES IN CASE OF MULTI-OBJECTIVE OPTIMIZATIONS.

Control Variable	Min	Max	Resolution	# of Cases	# of String
Gas Flow (kg/s)	400	650	0.1	2501	12
Compressor Flow Split (fraction to J Compressor)	0.15	0.55	0.001	401	9
J cooler cases	0	4	1	4	2
K cooler cases	0	4	1	4	2
J Cooler bypass fraction	0	1	0.01	101	7
K Cooler bypass fraction	0	1	0.01	101	7
Total String Length					**39**
Search Space					**5.50E+11**

NOx EMISSION MODEL

Predictive Emission Monitoring (PEM) models have been developed for non-DLE GE LM2500 and GE LM1600 gas turbines used on a natural gas compressor station on the TransCanada Pipeline System in Alberta. The PEM models are based on an optimized Neural Network (NN) architecture which takes four fundamental engine parameters as input variables [26-28]. These models predict NOx emission in ppmv-dry-O2 corrected and in kg/hr as NO2. The NN was trained using Continuous Emission Monitoring (CEM) measurements comprising sets of actual emission data collected over different seasons to capture the effects of ambient temperature variation. These training data were supplemented by other emission data generated by GE ‘Cycle-Deck’ tools to generate emission data at different ambient temperatures ranging from -30 to +30°C in the case of the LM2500, or Computational Fluid Dynamic simulation-generated data for the case of LM1600. The PEM models comprise a simple single hidden layer perceptron type NN with only two neurons in it, as shown in Fig. 9. The performance of the NN based model showed a correlation coefficient greater than 0.99, and error standard deviation of 1.1-1.4 kg/hr as NO2 [28]. Sensitivity analysis was conducted to assess the effects of uncertainties in the engine parameters on the NOx predictions by PEM. It was shown that for uncertainty in the ambient temperature of +1°C, the uncertainty in the NOx prediction is +0.9% to +3.5%. Uncertainties of the order of +1% in the other three input parameters results in uncertainties in NOx predictions by +2.5 to +6% [28]. Figures 10 and 11 show comparison between prediced vs. measured NOx emissions from a non-DLE GE LM2500 and LM1600 gas turbine, respectively.

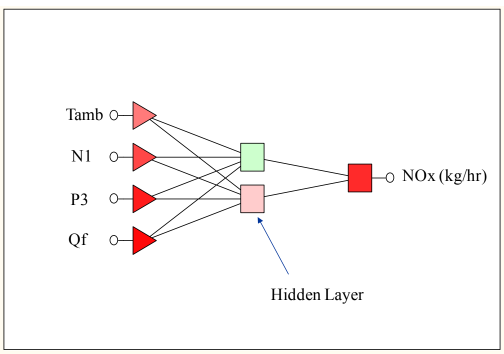

FIGURE 9: PEM NEURAL NETWORK BASED MODEL ARCHITECTURE.

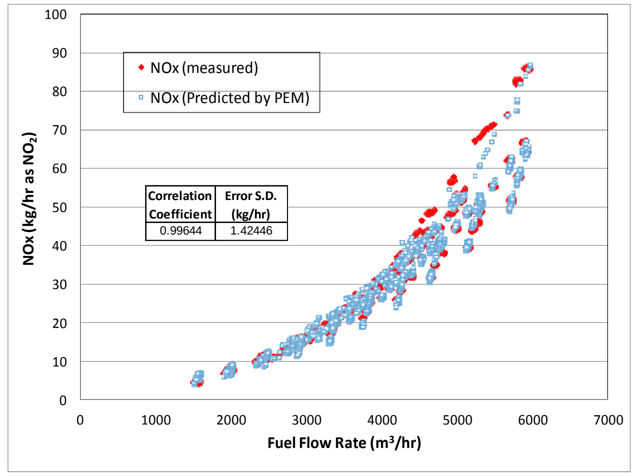

FIGURE 10: PEM MODEL PREDICTION VS. MEASURED NOx FOR A NON-DLE GE LM2500 GAS TURBINE.

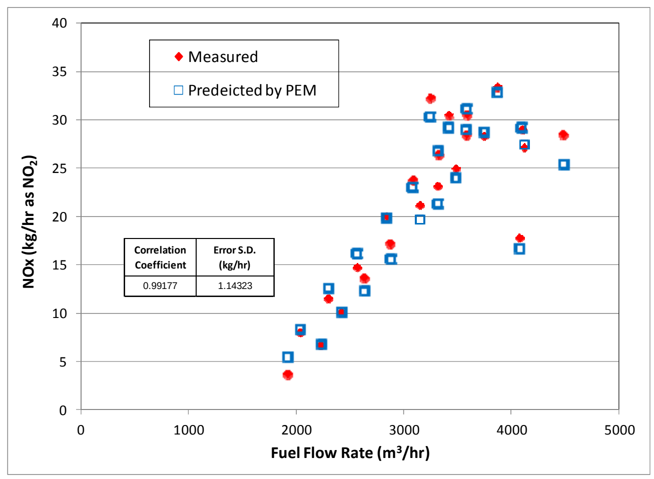

FIGURE 11: PEM MODEL PREDICTION VS. MEASURED NOx FOR A NON-DLE GE LM1600 GAS TURBINE.

GENETIC ALGORITHM PARAMETERS

Previous effort was devoted to determine the optimum set of GA operators. Combinatorial variations of these operators were examined and the resulting two-objective Pareto front characteristics were evaluated in terms of convergence to a stable non-dominated solution and diversity of the optimum cases along the converged Pareto front. The optimum set of the GA operators thus arrived at are given below:

- Elitism: 5%
- Copying: 5%
- Mutation: 10%

- Directional crossover: 50%
- Classical crossover: 30%

Effort has also been devoted to the optimum number of populations and generations to achieve convergence with minimum computational effort and without compromising the accuracy of the results. Experimenting with different scenarios resulted in a population size of 400 and 1000 for the single- and multi-objective runs, respectively. Convergence was obtained after 30 and 40 generations, respectively.

RESULTS OF TWO-OBJECTIVE OPTIMIZATIONS

Two-objective optimization simulations were conducted at two different fixed throughput of 511.7 kg/s (~2.1 BSCFD), and 600 kg/s (~2.46 BSCFD). The results for the 511.7 kg/s case are shown in Fig. 12, where the total energy consumption is shown on the x-axis and the NOx emission is on the y-axis. The Pareto points are also identified. The different colors correspond to different aerial coolers' scenario as indicated, which show that in order to achieve the absolute minimum NOx emission, a shift to more utilization of the aerial coolers with electric energy is required. This does not mean that a minimum total energy consumption is achieved. Clearly, there is a trade-off between the two as shown in Fig. 12. The resulting CO2e from this simulation is shown in Fig. 13. The CO2e is determined from the fuel flow consumption multiplied by an emission factor (EF) according to the following:

$$\text{EF} = 2.03 \text{ tonnes of CO2e per E3M3 of gas fuel} \qquad (8)$$

The above EF is based on combination of i) history of station; ii) AP42, iii) Stoichiometric combustion and iv) Global Warming Potential GWP (which is 21 × CH4 + 310 × N2O + 1 × CO2). Therefore, the CO2e emission tracks the fuel consumption via EF. Emissions associated with electrical production and the costs allocated to the resultant emissions were not included in the cost optimization of this study.

Figure 14 shows, again, the Pareto points on a smaller scale graph to identify six operating points that bracket the three different aerial cooler scenarios. The corresponding fuel and electric energy consumptions, as well as NOx and CO2e emissions are given in Table 6. These are also plotted as normalized parameters w.r.t. the minimum total energy consumption case (operating point #1) in Fig. 15. This Figure illustrates clearly that in order to realize minimum NOx and CO2e emissions, a trade-off has to occur between the electric energy consumed in the aerial cooler and the fuel energy used in the gas turbine, such that more utilization of the aerial cooler is required. However, it appears that the gain in lower NOx and CO2e emission is not that significant (about 1.2% reduction in NOx and 0.5% reduction in CO2e). Hence, optimizing for minimum total energy would be adequate, unless charges for NOx and CO2e emission are high.

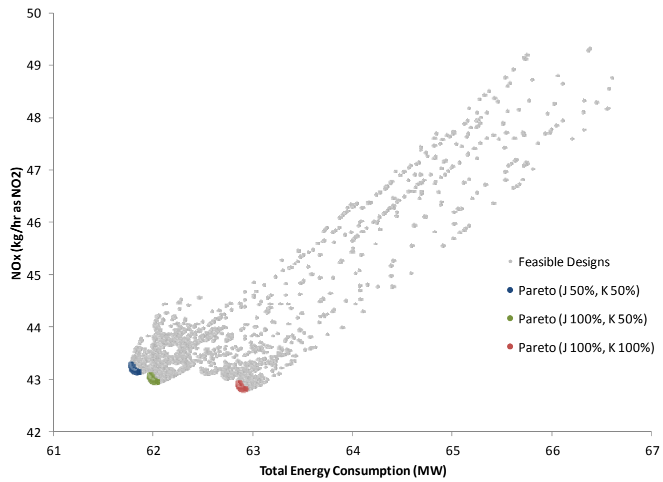

FIGURE 12: RESULTS OF TWO-OBJECTIVE OPTIMIZATION OF MINIMUM TOTAL ENERGY CONSUMPTION AND MINIMUM NOx EMISSION (THROUGHPUT = 511.7 kg/s).

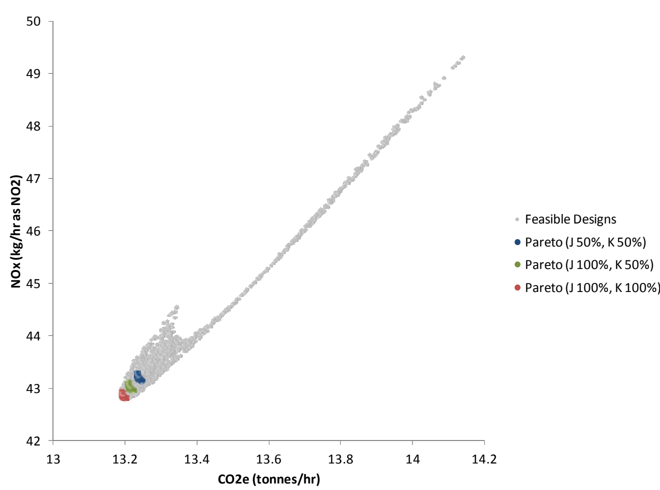

FIGURE 13: OPTIMIZED NOx EMISSION AND CORRESPONDING CO2E EMISSION FROM THE OPTIMIZATION DATA OF FIG. 12 (THROUGHPUT = 511.7 kg/s).

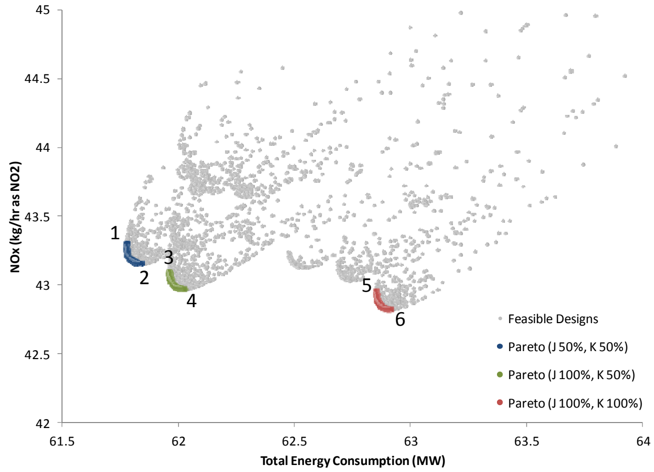

FIGURE 14: IDENTIFICATION OF SIX OPERATING POINTS ON THE PARETO FRONT FROM THE TWO-OBJECTIVE OPTIMIZATION OF MINIMUM TOTAL ENERGY CONSUMPTION AND MINIMUM NOx EMISSION (THROUGHPUT = 511.7 kg/s).

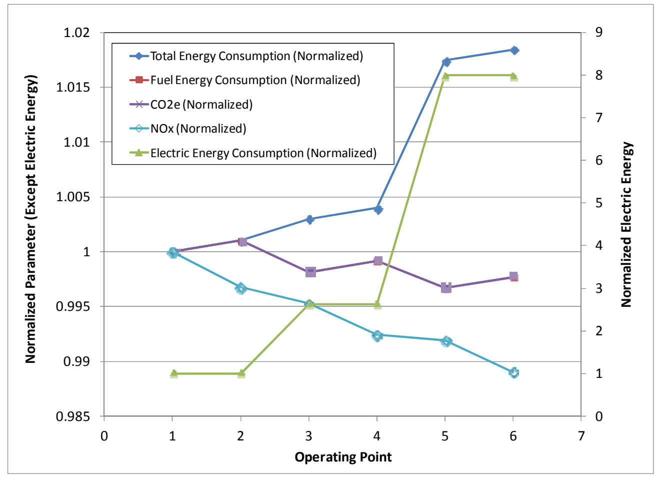

FIGURE 15: NORMALIZED ENERGY AND EMISSION PARAMETERS (WITH RESPECT TO THE MINIMUM TOTAL ENERGY CONSUMPTION CASE) OF THE SIX OPERATING POINTS ON THE PARETO FRONT FROM THE TWO-OBJECTIVE OPTIMIZATION OF FIG. 14 (THROUGHPUT = 511.7 kg/s).

TABLE 6 – ENERGY CONSUMPTION AND EMISSIONS OF THE IDENTIFIED SIX OPERATING POINTS ON THE PARETO FRONT FROM THE TWO-OBJECTIVE OPTIMIZATION OF MINIMUM TOTAL ENERGY CONSUMPTION AND MINIMUM NOx EMISSION (THROUGHPUT = 511.7 kg/s)

Operating Point	Total Energy Consumption (MW)	Fuel Energy Consumption (MW)	Electric Energy Consumption (MWe/0.3)	CO2e (tonnes/hr)	NOx (kg/hr)
1	61.772	61.589	0.183	13.230	43.306
2	61.835	61.652	0.183	13.244	43.165
3	61.956	61.476	0.481	13.206	43.102
4	62.019	61.539	0.481	13.219	42.979
5	62.849	61.385	1.464	13.186	42.955
6	62.911	61.447	1.464	13.200	42.830

In order to investigate the effects of emission charges on the optimization protocol, three different charges for CO2e and NOx emissions were applied (for argument sake). Figures 16, 17 and 18 show the normalized fuel and emission charges for the six optimum operating points on the Pareto front. The hypothetical emission charges are identified in each respective Figure. It is shown that the total charges (cost of energy + emission charges) are not lower than that of operating point #1, unless the emission charges are escalated, e.g. \$150/tonne of CO2e and \$16,000/tonne of NOx.

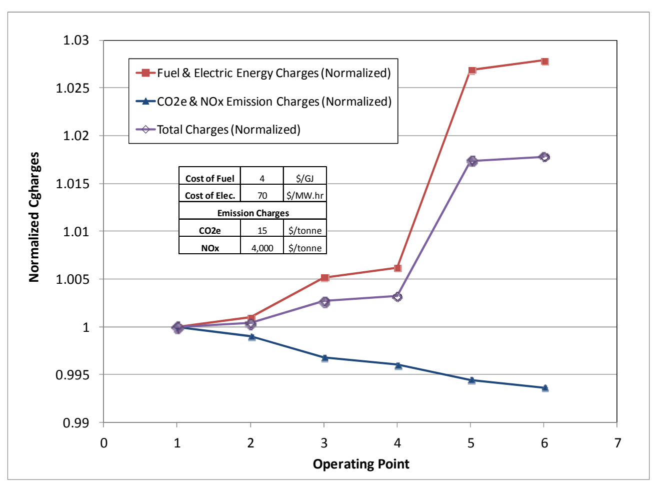

FIGURE 16: NORMALIZED ENERGY AND EMISSION CHARGES (WITH RESPECT TO THE MINIMUM TOTAL ENERGY CONSUMPTION CASE) OF THE SIX OPERATING POINTS ON THE PARETO FRONT ON FIG. 14 (EMISSION CHARGE SCHEME 1).

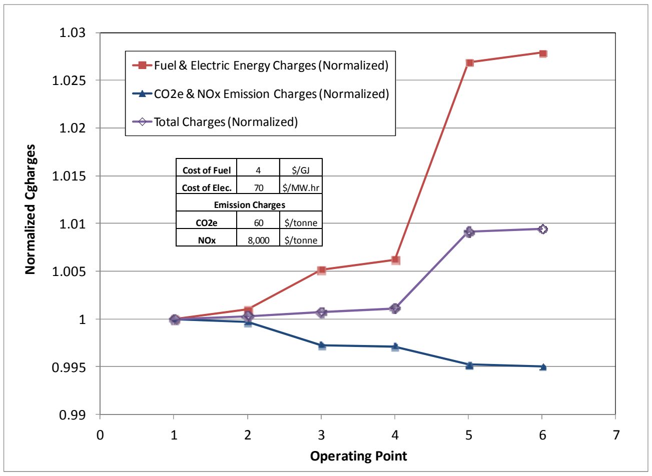

FIGURE 17: NORMALIZED ENERGY AND EMISSION CHARGES (WITH RESPECT TO THE MINIMUM TOTAL ENERGY CONSUMPTION CASE) OF THE SIX OPERATING POINTS ON THE PARETO FRONT ON FIG. 14 (EMISSION CHARGE SCHEME 2).

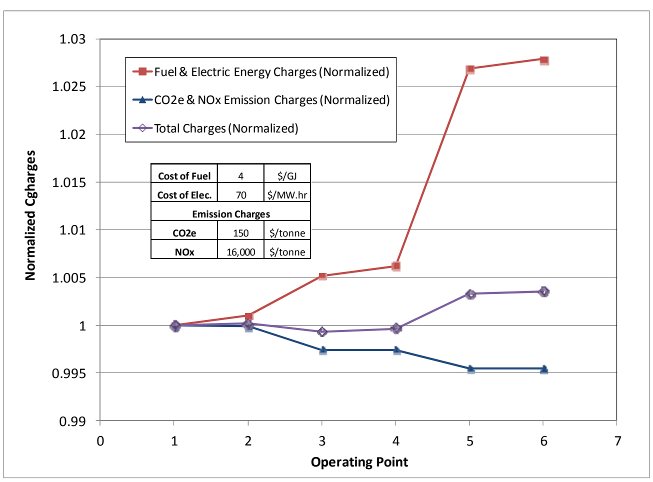

FIGURE 18: NORMALIZED ENERGY AND EMISSION CHARGES (WITH RESPECT TO THE MINIMUM TOTAL ENERGY CONSUMPTION CASE) OF THE SIX OPERATING POINTS ON THE PARETO FRONT ON FIG. 14 (EMISSION CHARGE SCHEME 3).

Similar results are shown for the higher throughput case of 600 kg/s. The corresponding results are shown in indicative Figures 19 through 25 and Table 7. For this throughput, the normalized fuel and emission charges for the six optimum operating points on the Pareto front show slightly lower total charges than that of point 1 as the emission charges are increased.

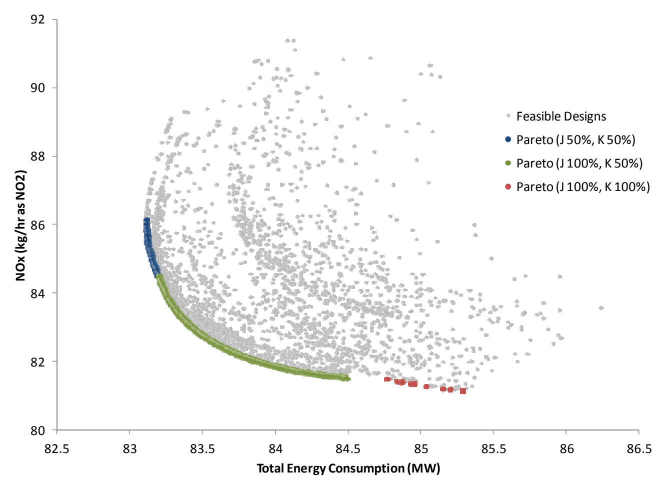

FIGURE 19: RESULTS OF TWO-OBJECTIVE OPTIMIZATION OF MINIMUM TOTAL ENERGY CONSUMPTION AND MINIMUM NOx EMISSION (THROUGHPUT = 600 kg/s).

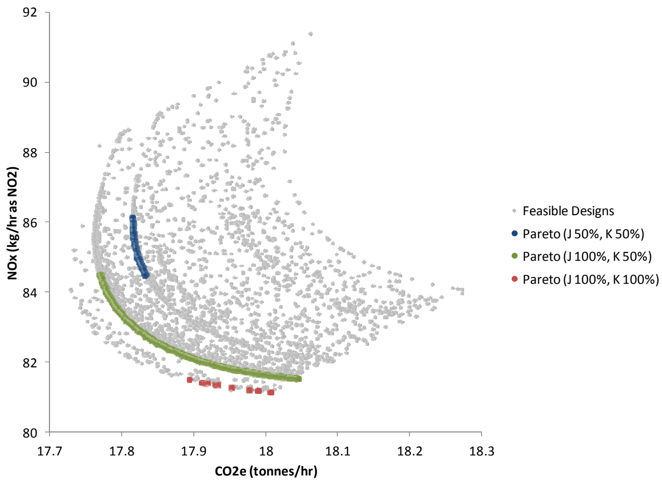

FIGURE 20: OPTIMIZED NOx EMISSION AND CORRESPONDING CO2E EMISSION FROM THE OPTIMIZATION DATA OF FIG. 8 (THROUGHPUT = 600 kg/s).

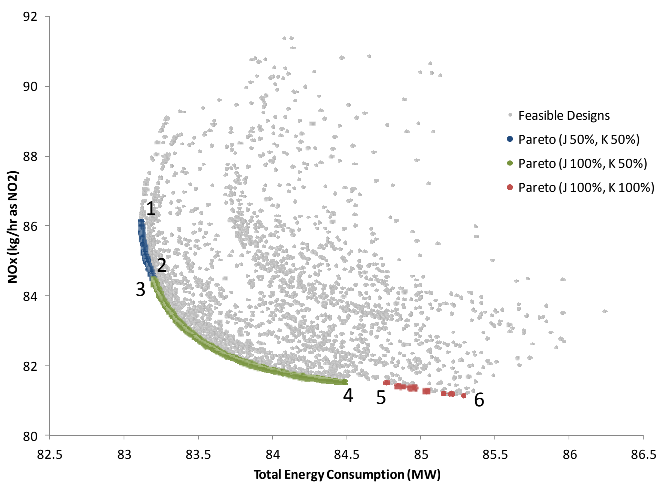

FIGURE 21: IDENTIFICATION OF SIX OPERATING POINTS ON THE PARETO FRONT FROM THE TWO-OBJECTIVE OPTIMIZATION OF MINIMUM TOTAL ENERGY CONSUMPTION AND MINIMUM NOx EMISSION (THROUGHPUT = 600 kg/s).

TABLE 7: ENERGY CONSUMPTION AND EMISSIONS OF THE IDENTIFIED SIX OPERATING POINTS ON THE PARETO FRONT ON FIG. 21

Operating Point	Total Energy Consumption (MW)	Fuel Energy Consumption (MW)	Electric Energy Consumption (MWe/0.3)	CO2e (tonnes/hr)	NOx (kg/hr)
1	83.107	82.924	0.183	17.813	86.146
2	83.194	83.011	0.183	17.832	84.492
3	83.193	82.713	0.481	17.768	84.510
4	84.474	83.994	0.481	18.043	81.559
5	84.758	83.294	1.464	17.893	81.524
6	85.279	83.815	1.464	18.005	81.177

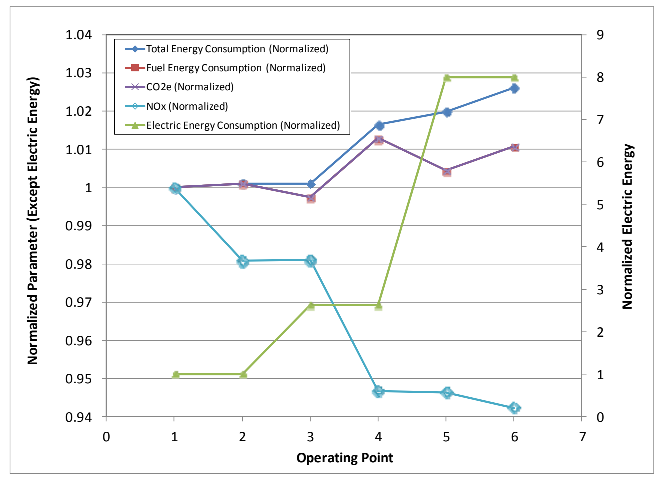

FIGURE 22: NORMALIZED ENERGY AND EMISSION PARAMETERS (WITH RESPECT TO THE MINIMUM TOTAL ENERGY CONSUMPTION CASE) OF THE SIX OPERATING POINTS ON THE PARETO FRONT ON FIG. 21.

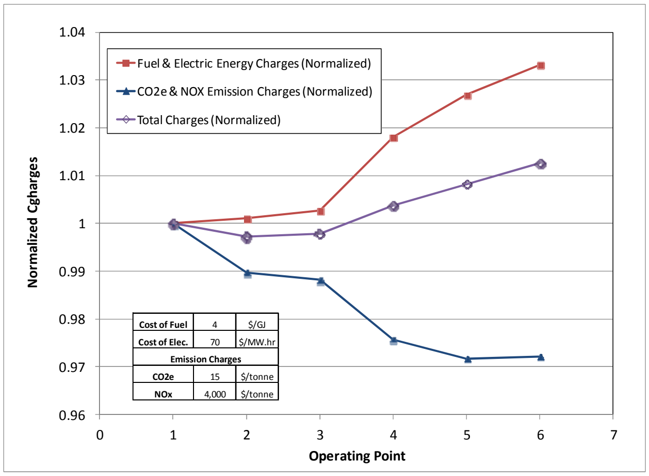

FIGURE 23: NORMALIZED ENERGY AND EMISSION CHARGES (WITH RESPECT TO THE MINIMUM TOTAL ENERGY CONSUMPTION CASE) OF THE SIX OPERATING POINTS ON THE PARETO FRONT FROM ON FIG. 21 (EMISSION CHARGE SCHEME 1).

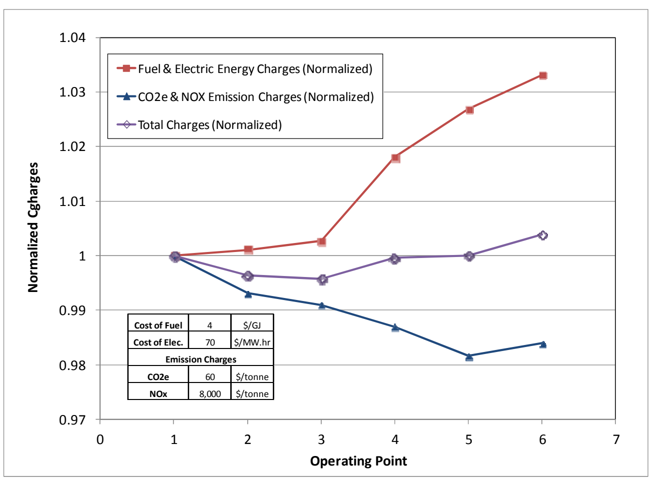

FIGURE 24: NORMALIZED ENERGY AND EMISSION CHARGES (WITH RESPECT TO THE MINIMUM TOTAL ENERGY CONSUMPTION CASE) OF THE SIX OPERATING POINTS ON THE PARETO FRONT ON FIG. 21 (EMISSION CHARGE SCHEME 2).

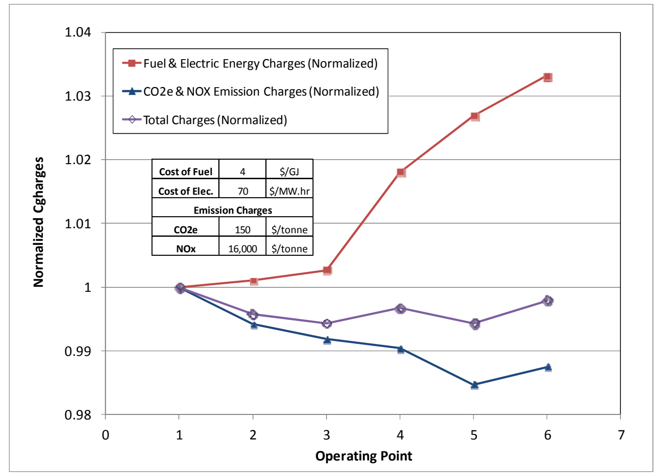

FIGURE 25: NORMALIZED ENERGY AND EMISSION CHARGES (WITH RESPECT TO THE MINIMUM TOTAL ENERGY CONSUMPTION CASE) OF THE SIX OPERATING POINTS ON THE PARETO FRONT ON FIG. 21 (EMISSION CHARGE SCHEME 3).

CONCLUSIONS

The following conclusions can be drawn from the present investigation:

1. Savings in the energy consumption is achievable with slight adjustment to unit load sharing and coolers by-pass/fan speed selections. It appears that most of the savings (around 70–75%) are derived from optimizing the load sharing between the two parallel compressors, while the balance of the savings is realized from optimizing the aerial coolers settings.

2. In order to minimize either NOx or CO2e directly attributed to the pipeline system, a shift towards maximum electric usage is required, i.e. maximum utilization of aerial coolers. This is not necessarily the best or optimum scenario from total energy consumption.

3. If emission charges are up to \$60/tonne CO2e and \$8,000 /tonne NOx, there is no benefit in optimizing for either CO2e or NOx. Minimum total energy consumption corresponds to minimum overall cost (energy and emission). This of course depends on fuel and electric energy costs.

4. If emission charges are up to \$150/tonne CO2e and \$16,000 /tonne NOx, there could be benefits in optimizing for both. Minimum total energy consumption is not necessarily the minimum cost scenario in this case.

ACKNOWLEDGMENT

The multi-objective genetic algorithm (MOGA) optimization software used in the present work was modeFRONTIER by ESTECO [29] which is hereby acknowledged. The characteristics of the aerial coolers shown in Figures 3 through 6 were obtained using aspenONE V7.0 (Engineering Software EDR). The present work is part of a research program sponsored by TransCanada PipeLines Limited, and permission to publish it is hereby acknowledged.

REFERENCES

[1] Botros, K.K., Sennhauser, D.J., Stoffregen, J., Jungowski, K. and Golshan, H.: "Large Pipeline Network Optimization – Summary and Conclusions of TransCanada Research Effort", 6th International Pipeline Conference, Calgary, Alberta, Canada, September 25-29, 2006.

[2] Stoffregen, J., Botros, K.K., Sennhauser, D.J., Jungowski, K. and Golshan, H.: "Large Pipeline Network Optimization – A Practical and Technical Assessment", 37th PSIG Annual Meeting, San Antonio, TX, November 7-9, 2005.

[3] Botros, K.K., Sennhauser, D.J., Jungowski, K., Poissant, G., Golshan, H. and Stoffregen, J.: "Effects of Dynamic Penalty Parameters on the Conversion of MOGA in Optimization of a Large Gas Pipeline Network", 10th AIAA/ISSMO Multidisciplinary Analysis and Optimization Conference, Albany, New York, Aug 30 – 1 September, 2004.

[4] Botros, K.K., Sennhauser, D.J., Jungowski, K., Poissant, G., Golshan, H. and Stoffregen, J.: "Multi-objective Optimization of Large Pipeline Networks Using Genetic Algorithm", International Pipeline Conference, Calgary, Alberta, Canada, October 4-8, 2004.

[5] Hawryluk, A., Botros, K.K., Golshan, H. and Huynh, B.: "Multi-Objective Optimization of Natural Gas Compression Power Train with Genetic Algorithms", ASME 8th International Pipeline Conference & Exhibition, TELUS Convention Centre, Calgary, Alberta, Canada, September 27- through October 1, 2010.

[6] Boyd, E.A. and Scott, L.R.: "Evaluating the Quality of Pipeline Optimization Algorithms", *Pipeline Simulation Interest Group,* 29th Annual Meeting, 1997.

[7] Carter, R.G.: "Compressor Station Optimization: Computational Accuracy and Speed", Pipeline Simulation Interest Group, 28th Annual Meeting, San Francisco, CA, October 24-25, 1996.

[8] Goslinga, J., Kaulback, M., Witczak, K. and McNeill, B.: "A Method for Pipeline Network Optimization", ASME Offshore Mechanics and Arctic Engineering, Volume V, Pipeline Technology, pp.31-43, 1994.

[9] Osiadacz, A.J. and Bell, D.J.: "Simplified Algorithm For Optimization Of Large-Scale Gas Networks", Optimal Control Applications and Methods, Vol. 7, pp. 95-104, 1986.

[10] Rachford, Jr. H.H. and Carter, R. G.: "Optimizing Pipeline Control In Transient Gas Flow", Pipeline Simulation Interest Group, 32nd Annual Meeting, 2000.

[11] Shaw, D.C.: "Pipeline System Optimization: A Tutorial", Pipeline Simulation Interest Group, 26th Annual Meeting, San Diego, CA, October, 1994.

[12] Sung, W., Huh, D., Lee, J. and Kwon, O.: "Optimization of Pipeline Networks with a Hybrid MCST-CD Networking Model", SPE Production and Facilities, pp. 213-219, August 1998.

[13] Wilson, J.G., Mallinson, J.R. and Ceney, J.E.: "Simulation and Optimization of Gas Transmission Systems", Int. Gas Research Conference, pp.373-385, 1986.

[14] Percell, P.B. and Ryan, M.J.: "Steady-State Optimization of Gas Pipeline network Operation", Pipeline Simulation Interest Group, Annual Meeting, Tulsa, Oklahoma, October 22-23, 1987.

[15] More, J.J. and Wright, S.J., Optimization Software Guide, Society for Industrial and Applied Mathematics, Philadelphia, 1993.

[16] Pietsch, U., Rachford H.H. and Carter R.G.: Investigating Real-World Applications of Transient Optimization, Pipeline Simulation Interest Group, 2001.

[17] Rachford, H.H. and Carter R.G.: Optimizing Pipeline Control in Transient Gas Flow", Pipeline Simulation Interest Group, 2000.

[18] Sood, A.K., Funk,G.L. and Delmastro, A.C.: "Dynamic Optimization of a Natural Gas Pipeline Using a Gradient Search Technique", Int. Journal of Control, Vol. 14, No. 6, pp. 1149-1157, 1971.

[19] Tsal, R.J., Gordon, E., Simpson, K.O. and Olson, R. R.: "Optimal Gas Pipeline Design via Dynamic Programming with Variable Stages", Pipeline Simulation Interest Group, Annual Meeting, New Orleans, LA, October 30-31, 1988.

[20] Short, M. and Meller, S.H.: "Elements of Comprehensive Pipeline Optimization", International Pipeline Conference, Volume 2, pp. 1211-1220, 1996.

[21] Bolkan, Y.G., Mehrotra, A.K. and Hastaoglu, A.M.: "Development of an Efficient Algorithm for Optimal Pipeline Design and Operation", ASME Offshore Mechanics and Arctic Engineering, Volume V-B, Pipeline Technology, pp.517-524, 1992.

[22] Goldberg, D.E. and Kuo, C.H.: "Genetic Algorithms in Pipeline Optimization", Pipeline Simulation Interest Group, Annual Meeting, Albuquerque, New Mexico, October 24-25, 1985.

[23] Goldberg, D. E.," Computer-Aided Pipeline Operation Using Genetic Algorithms and Rule Learning. Part I: Genetic Algorithm in Pipeline Optimization", Engineering with Computers, Vol 3 (1), pp. 35-45, 1987.

[24] Yandong S. and Pingyuan, X, "Genetic algorithm and gradient-based algorithm optimization of vehicle turning mechanism," ICCSIT, pp.81-84, 2009, 2nd IEEE International Conference on Computer Science and Information Technology, 2009.

[25] Starling, K.E. and Savidge, J.L.: "Compressibility Factors for Natural Gas and Other Related Hydrocarbon Gases", American Gas Association, Transmission Measurement Committee Report No. 8., 1992.

[26] Botros, K.K., Price, G.R. and Kibrya, G.: "Predictive Emission Monitoring Model For LM1600 Gas Turbines Based On Neural Network Architecture Trained on Field Measurements and CFD Data", the 46th ASME Gas Turbine and Aeroengine Congress, Exposition, and Users Symposium, paper #2001-GT-0221, New Orleans, Louisiana, June 4-7, 2001.

[27] Price, G.R.; Botros, K.K. and Goldin, G.M.: "CFD Predictions and Field Measurements of NOx Emissions From LM1600 Gas Turbine During Part Load Operation", Transactions of the ASME, Journal of Engineering for Gas Turbines and Power, v. 124, pp. 276-283, 2002.

[28] Botros, K.K. and Cheung, M.: "Neural Network Based Predictive Emission Monitoring Module for a GE LM2500 Gas Turbine", ASME 8th International Pipeline Conference & Exhibition, TELUS Convention Centre, Calgary, Alberta, Canada, September 27- through October 1, 2010.

[29] ESTECO srl (2007). ModeFRONTIER (optimization software system), version 3.2.2, http://www.esteco.com/products.jsp.